2

MPL TECHNICAL MEMORANDUM 279

6 ELEMENT LOCATION FOR THE ADA ARRAY

10 V. C./Anderson

University of California, San Diego
Marine Physical Laboratory of the
Scripps Institution of Oceanography
San Diego, California 92132

12 20

11 14 January 1977

9 Technical memo.

Sponsored by
Advanced Research Projects Agency
ARPA Order Number 2426
Program Code Number 62702E

15

Administered by the Office of Naval Research
Contract N00014-75-C-0108, new
ARPA Order-2426

Scientific Officer: Director, ~~Sensor Technology~~ Projects Division
Technology Directorate
Office of Naval Research
Department of the Navy

14 MPL-TM-279
MPL-U-43/76

MPL-U-43/76
TM 279

ELEMENT LOCATION FOR THE ADA ARRAY

V. C. Anderson

The structure of the hydrophone element mounts used in the ADA array may lead to slow changes in the actual element locations during the operating period and, in particular, during the ascent and descent operations when significant changes in temperature and in structural stress in the pressure hull can occur. In view of this, we intend to implement an acoustic element location system which can monitor the positions of the elements in nearly real-time.

The approach to the localization system is to establish a base-line array of high frequency reference transducers around the periphery of the array. This set will be rigidly coupled to the deck so that the locations can be measured during installation and can be assumed to be stable within the required tolerance. This will clearly be true with respect to distances along the deck, but some curvature or deformation could occur over the full length of the deck in what will be called the "z" axis. A series of bootstrap calibrations down the full length of the array will hopefully measure any such deformation. If the cumulative error in such a measurement proves to be too large, data can be derived from observation of a distant source with a number of selected elements whose local relative geometry has been determined by the nearfield calibration system.

The high frequency base-line array will be used to survey in the instantaneous locations of dual-frequency calibration sources suspended over the array on the inner surface of the protective fabric dome. The construction of these

sources is sketched in Fig. 1. The 1 inch cylinders are resonant at 40 kHz, in the circumferential mode of oscillation and couple in their interior to a 1/4 lambda resonant chamber operating at 2.5 kHz. They are pulsed at 40 kHz for localization with respect to the base-line array and then are operated in the continuous mode at 2.5 kHz. For phase localization of the elements the sources are sequenced in time so that phase arrivals from the different calibration sources can be measured without mutual interference.

The following analysis indicates that a set of 6 transducers in the base-line array and 6 dual frequency calibration sources will suffice to measure the element locations to a precision of + - .2 radians at 2.5 kHz. This will limit the degredation of the array pattern on axis due to the uncertainties of the element locations to less than .1 dB. This assumes the dominant error to be in the phase measurement at 2.5 kHz and that the phase measurement error will be less then ± .1 radians.

THE LOCATION ALGORITHM

We assume three fixed points, whose positions are known, the velocity of sound to be known, and one unknown point not located in the plane of the three reference points. The constants in the problem then are the nine coordinates of the known points and the velocity of sound. The data are the three travel times between the known and unknown points. The basic travel time equations are:

$$C^2 T_j^2 = (x - x_j)^2 + (y - y_j)^2 + (z - z_j)^2 . \tag{1}$$

using a Taylor's expansion,

$$C^2T_j^{\,2} = (x_0 - x_j)^2 + 2(x_0\ x_j)\Delta x + \cdots + (y_0 - y_j)^2 + 2(y_0 - y_j)\Delta y + \cdots + (z_0 - z_j)^2 + 2(z_0 - z_j)\Delta z \tag{2}$$

where x_0 is the estimated position $x = x_0 + \Delta k$ is the true position.

The set of equations can be expressed in matrix form as

$$\underline{A} \cdot \underline{X} = \underline{Y}$$

where

$$\underline{X} \left| \begin{array}{c} x \\ y \\ z \end{array} \right| , \quad \underline{A} = \left| \begin{array}{c} x_0 - x_1,\ y_0 - y_1,\ z_0 - z_1 \\ x_0 - x_2,\ y_0 - y_2,\ z_0 - z_2 \\ x_0 - x_3,\ y_0 - y_3,\ z_0 - z_3 \end{array} \right| , \quad \underline{Y} = \left| \begin{array}{c} (C^2T_1 - R_1^{\,2})/2 \\ (C^2T_2 - R_2^{\,2})/2 \\ (C^2T_3 - R_3^{\,2})/2 \end{array} \right|$$

and

$$R_j^{\,2} = (x_0 - x_j)^2 + (y_0 - y_j)^2 + (z_0 - z_j)^2 \tag{3}$$

solving the equation for $\underline{X}$

$$\underline{X} = \underline{A}^{-1} \cdot \underline{Y}\,. \tag{4}$$

Cramer's rule is used for the matrix inversion rather than the somewhat more efficient Gauss's expansion because it is more robust in an automated computation in that it avoids the possibility of dividing by a very small or zero coefficient, an event that plays havoc with the dynamic range of a computer. Cramer's rule as used is:

$$x_i = \frac{1}{|A|} \sum_{k=1}^{3} A'_{ki} y_{kj} \tag{5}$$

$|A|$ is the determinant of $\underline{A}$, A_{ki} is the cofactor of a_{ki}, the element of matrix $\underline{A}$, and Y_k is an element of vector $\underline{Y}$. The determinant is computed using Laplace's development,

$$|A| = a_{11}A_{11}^{1} + a_{22}A_{22}^{2} + a_{33}A_{33}^{1} . \tag{6}$$

In the computer algorithm the magnitude of the determinant is constrained to be larger than some arbitrary limit.

Appendix I is a listing of the subroutine for the solution using Equation 5 and 6. A modified routine is listed in Appendix II which constrains the maximum excursion of the correcting terms. In both of these algorithms a generally slightly higher rate of convergence is achieved by the use of a gain factor applied to the correcting terms.

Convergences for several cases are illustrated in Fig. 2. The upper curve represents the extreme case where the estimate is placed in the plane of the reference transducers. The determinant in this case is, of course, zero and the initial excursion is finite only because of the constraint on the minimum size of the determinant. The effect of the additional excursion constraints of II is apparent in the central cluster of curves. The number of iteration steps is reduced by 30% by virtue of these constraints. However, because of the additional computation required for the constraint, the overall processing time is actually longer for program II.

The gain factor of 1.1 shows a significant advantage in the convergence of these central curves, but not for the lower left hand ones with a different

and smaller displacement for the initial estimate. Here the gain factor actually reduces the convergence rate slightly.

LOCATION ERRORS

The statistics of the errors engendered by noise or instrumental degradation of the time delay data can be determined by differentiating Equation 5

$$x_j = 1/|A| \sum_{k=1}^{3} A^1_{kj} y_k = F_j(T_1, T_2, T_3)$$

$$dx_j = \alpha F_j / \alpha T_1 \, dT_1 + \alpha F_1 / \alpha T_2 \, dT_2 + \alpha F_j / \alpha T_3 \, dT_3$$

Assuming the dT's to be independent zero-mean random numbers of equal variance,

$$\sigma j^2 = ((\alpha F_j / \alpha T_1)^2 + (\alpha F_j / \alpha T_2)^2 + (\alpha F_j / \alpha T_3)^2) \, \sigma_T^2$$

$$\sigma j / \sigma_T = (1/|A|)((A^1_{1j} R_1)^2 + (A^1_{2j} R_2)^2 + (A^1_{3j} R_3)^2)^{1/2}$$

This ratio, the ratio of the location error in the x_j coordinate to the time delay error, is dependent on the geometry of the problem.

Figures 3 and 4 display error ratio contours in a plane of height Z_0 = .3, 0.3 times the reference array spacings. From these contours it is apparent that, over the x-y aperture of the reference array, the error ratio in the xy plane at a height of .3, corresponding approximately to the ADA geometry,

w ll be less than 2.0, and less than 1.0 over most of the aperture. The z error ratio will be less than 1.0 over the reference array aperture. Notice that the error ratio increases rapidly for locations beyond the limits of the aperture, the z error ratio increasing much more rapidly than that in the xy plane. The reason is, of course, that z is being measured more nearly endfire to the array. As a matter of fact, it is the coupling of the z error into the xy coord nate estimates that gives rise to the rapid increase in the xy error beyond the reference aperture boundary.

For comparison purposes the error contours for $z_0 = 1.0$ are shown in Figs. 5 and 6.

PHASE LOCATION

Once the dual-frequency calibration sources have been located using high frequency pulsed measurement of travel time, they are operated in the low frequency continuous mode for location of the main array elements. In this case, where the location is accomplished by the use of steady state sinusoidal signals, measuring the phase at an array element from a succession of source locations, the above algorithm can be used to obtain corrected positions. One way of accomplishing this is to convert the phase measurement to a time delay error as follows.

The phase from the j^{th} source is represented by

$$\mathrm{EXP}\,(i\,\phi_j) = \mathrm{COS}\,(\phi_j) + i\,\mathrm{SIN}\,(\phi_j) = \mathrm{EXP}\,(i\,\omega\,T_j)$$

The difference between the phase received with time delay and that which would have been observed for the range to the estimated position is,

$$\mathrm{EXP}(i\omega T_j - kR_j) = \mathrm{COS}(\phi_j)\mathrm{COS}(kR_j) + \mathrm{SIN}(\phi_j)\mathrm{SIN}(kR_j) + i(\mathrm{SIN}(\phi_j)\mathrm{COS}(kR_j) - \mathrm{COS}(\phi_j)\mathrm{SIN}(kR_j))$$

The difference $\Delta = \omega T_j - kR_j$ is then, within an ambiguity of $\pm\pi$,

$$\Delta = \omega T_j - kR_j = \mathrm{SIN}^{-1}(\mathrm{SIN}(\phi_j)\mathrm{COS}(kR_j) - \mathrm{COS}(\phi_j)\mathrm{SIN}(kR_j))$$

and also, to remove ambiguities,

$$\Delta = \omega T_j - kR_j = \mathrm{COS}^{-1}(\mathrm{COS}(\phi_j)\mathrm{COS}(kR_j) + \mathrm{SIN}(\phi_j)\mathrm{SIN}(kR_j))$$

The elements of the vector $\underline{Y}$ of Equation 4 can be approximated more directly, if $cT_j - R_j \angle\angle cT_j + R_j$ by,

$$\frac{C^2T_j - R_{0j}^2}{2} \simeq R_{0j}(CT_j - R_{0j}) = CR_{0j} \cdot \frac{\Delta}{\omega}$$

Subroutines for the phase rotation and conversion of phase components into time delay values are given in Appendix 3. The lookup tables used in these routines are sized to maintain an rms error of less than .003 wavelengths. The rotation subroutine also includes provision for the correction of constant phase shift offsets of an instrumental nature.

VELOCITY OF SOUND

It will be necessary to monitor the velocity of sound in the water inside of the dome because variations with temperature can be significant over the

range of temperatures which may be experienced in operation. Pairs of the base-line reference array elements may be used for this purpose, however, careful attention must be paid to their location to assure that a reliable path exists between the elements in the horizontal direction. This means that, first of all, the elements should be positioned at a height of 18 inches off the deck so that they will be in the first maximum of the Lloyd mirror interference pattern. Second, there should be no main array elements in the line-of-sight between the elements to be used for velocity of sound measurement.

As a very useful check on overall instrumental time delay offset it will be helpful to install an additional high frequency transducer immediately adjacent to one of the reference elements.

A suggested configuration for the high frequency reference array transducers is sketched in Fig. 7.

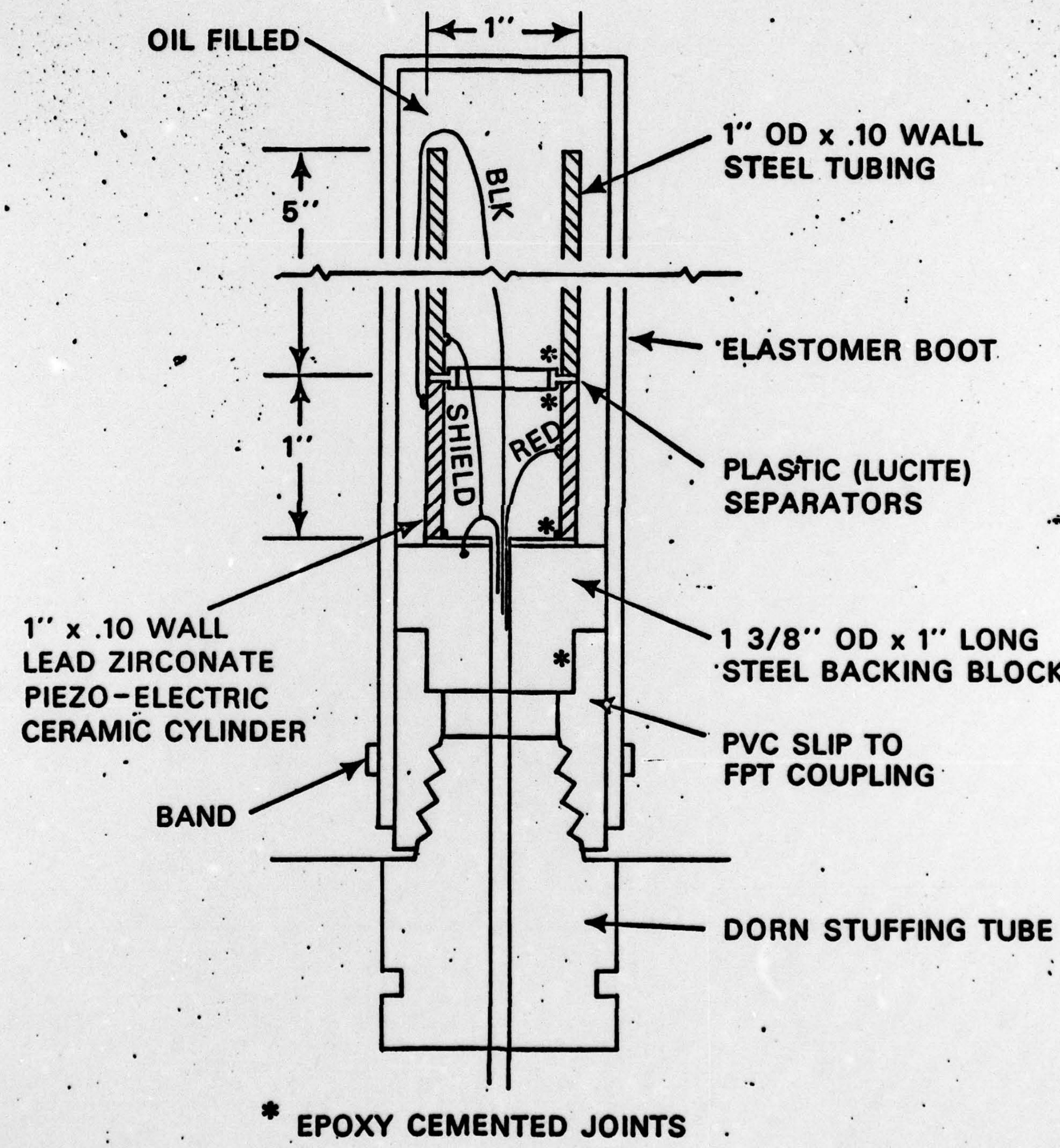

OIL FILLED
1"
1" OD x .10 WALL
STEEL TUBING
BLK
5"
ELASTOMER BOOT
SHIELD
RED
1"
PLASTIC (LUCITE)
SEPARATORS
1" x .10 WALL
LEAD ZIRCONATE
PIEZO-ELECTRIC
CERAMIC CYLINDER
1 3/8" OD x 1" LONG
STEEL BACKING BLOCK
PVC SLIP TO
FPT COUPLING
BAND
DORN STUFFING TUBE
* EPOXY CEMENTED JOINTS

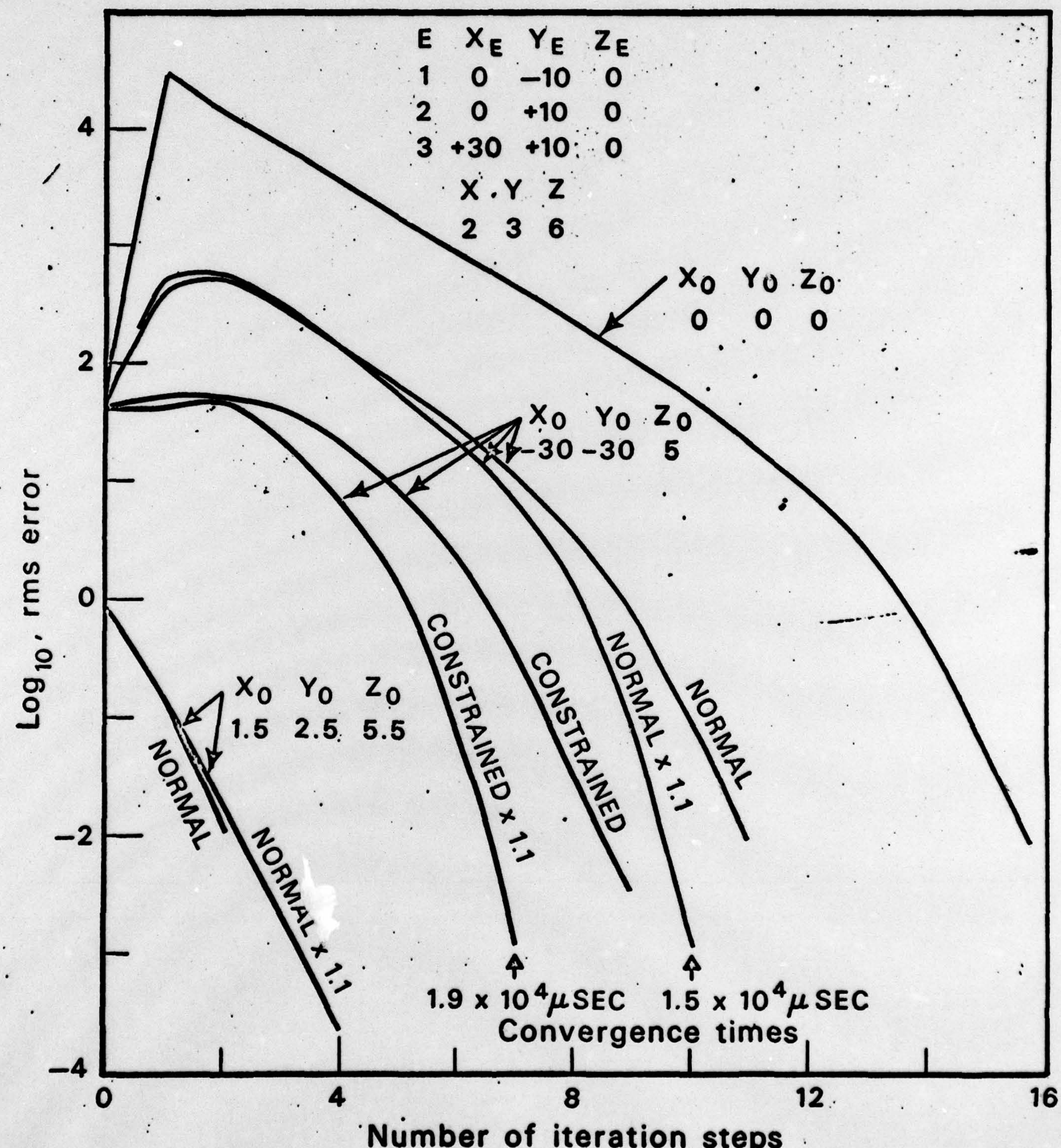

E XE YE ZE
1 0 −10 0
2 0 +10 0
3 +30 +10 0
X Y Z
2 3 6
X0 Y0 Z0
0 0 0
X0 Y0 Z0
−30 −30 5
X0 Y0 Z0
1.5 2.5 5.5
NORMAL
NORMAL x 1.1
CONSTRAINED x 1.1
CONSTRAINED
NORMAL x 1.1
NORMAL
1.9 x 10^4 μSEC
1.5 x 10^4 μSEC
Convergence times
Log10, rms error
Number of iteration steps
4
2
0
−2
−4
0
4
8
12
16

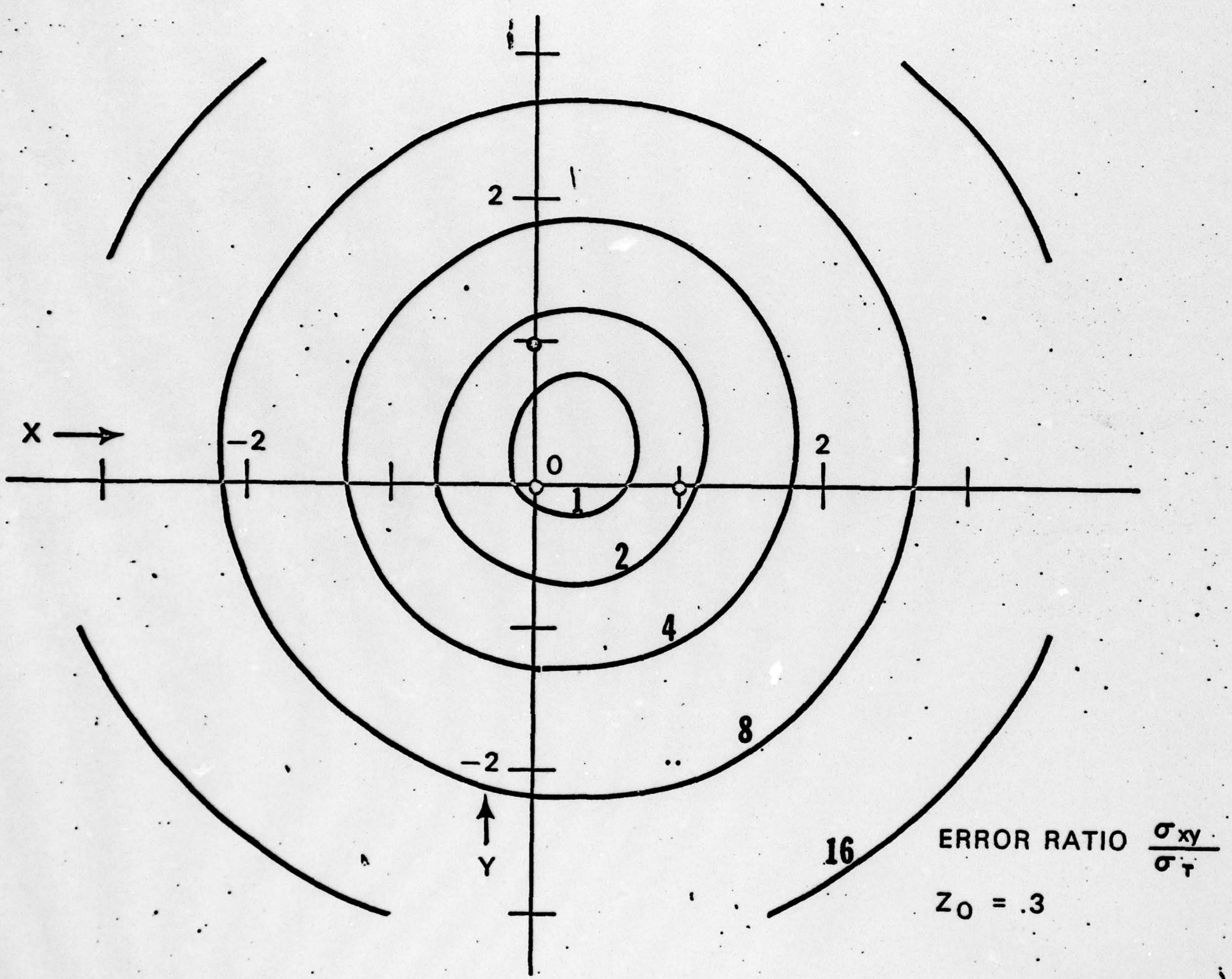

ANDERSON: FIG. 3
PL-M-4023(U)/RAPP 12/1/76

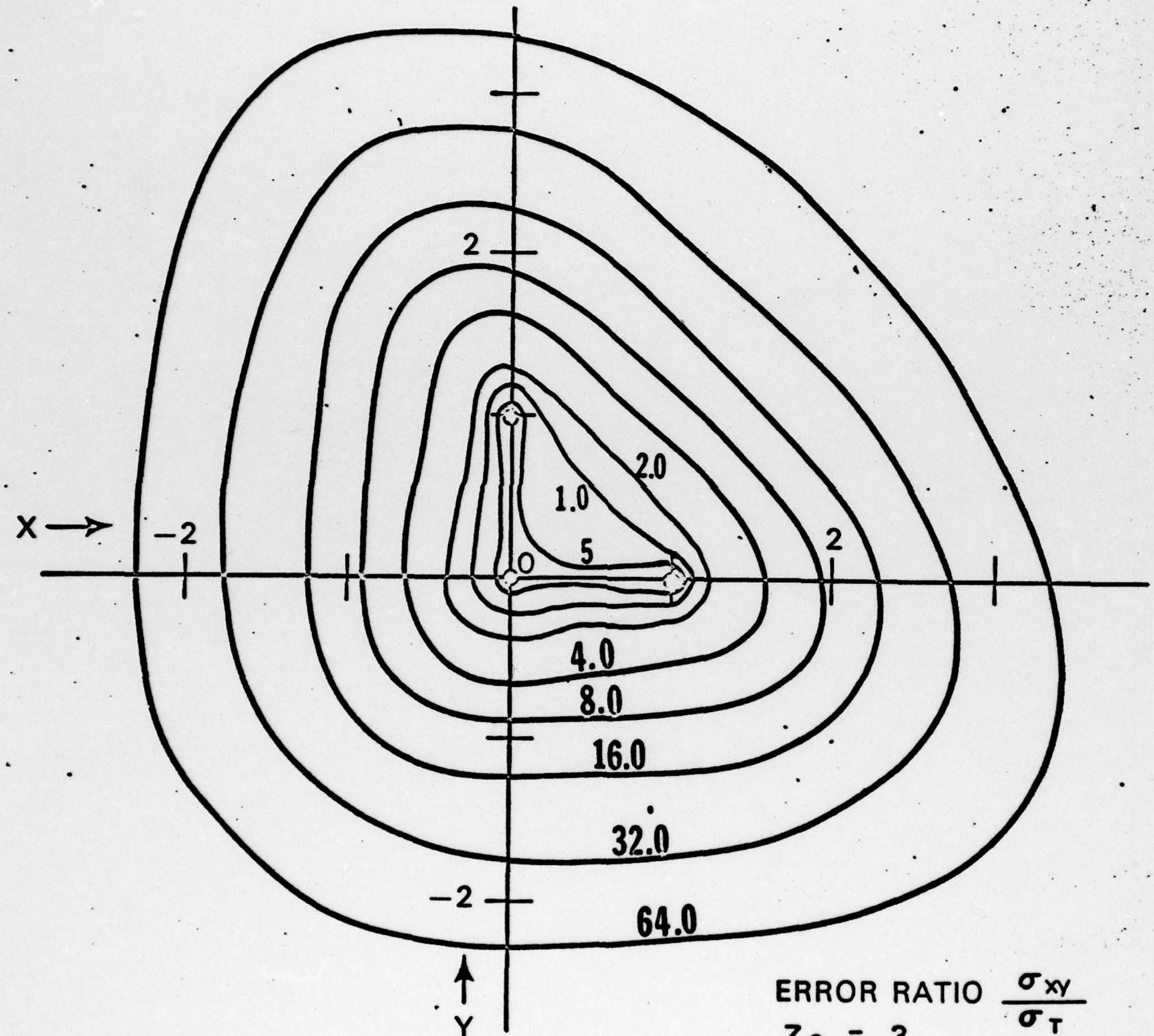

ERROR RATIO $\frac{\sigma_{XY}}{\sigma_T}$

$Z_0 = .3$

ANDERSON: FIG. 4
PL-M-4024(U)/RAPP 12/1/76

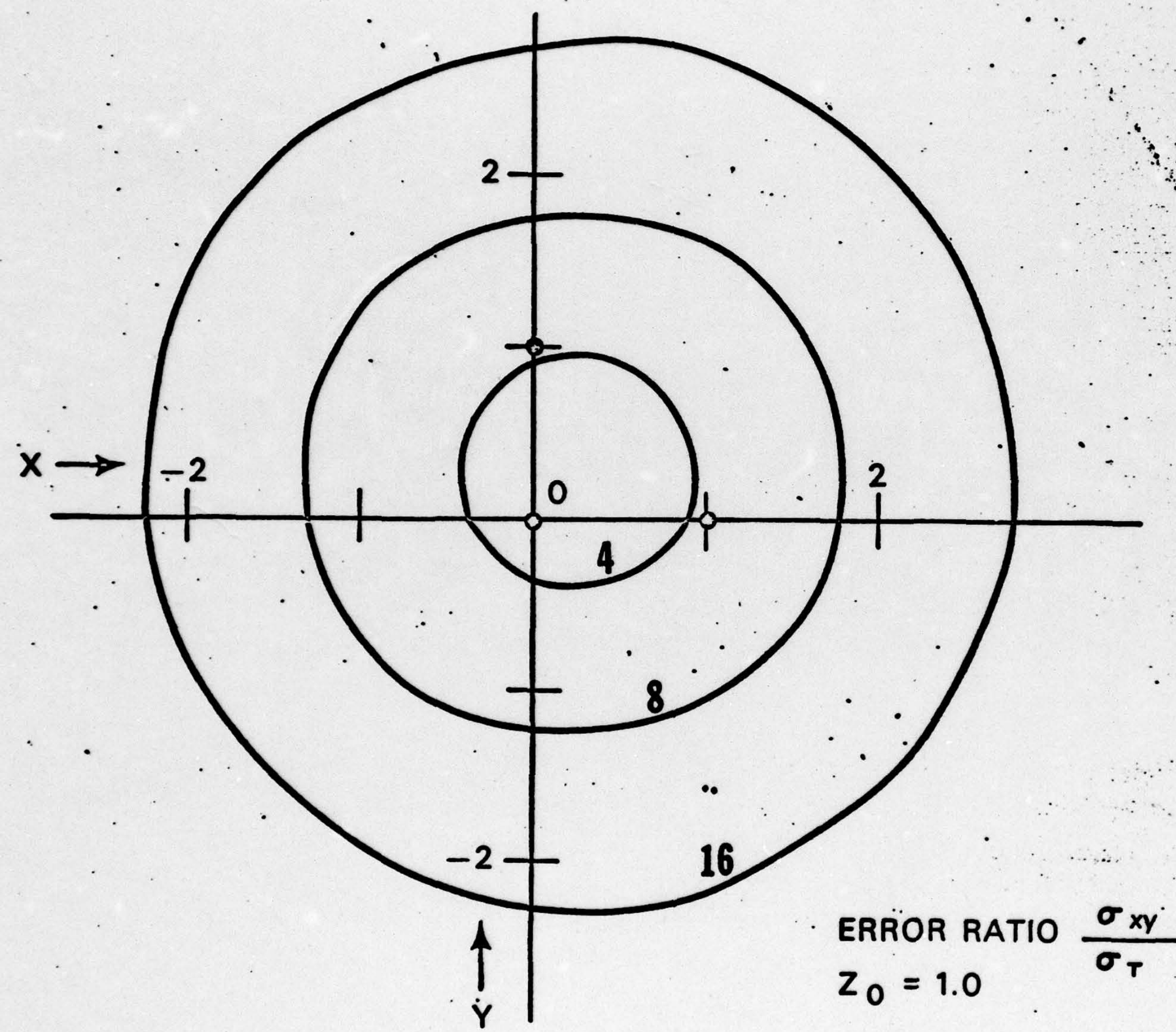

ANDERSON: FIG. 5
MPL-M-4025(U)/RAPP 12/1/76

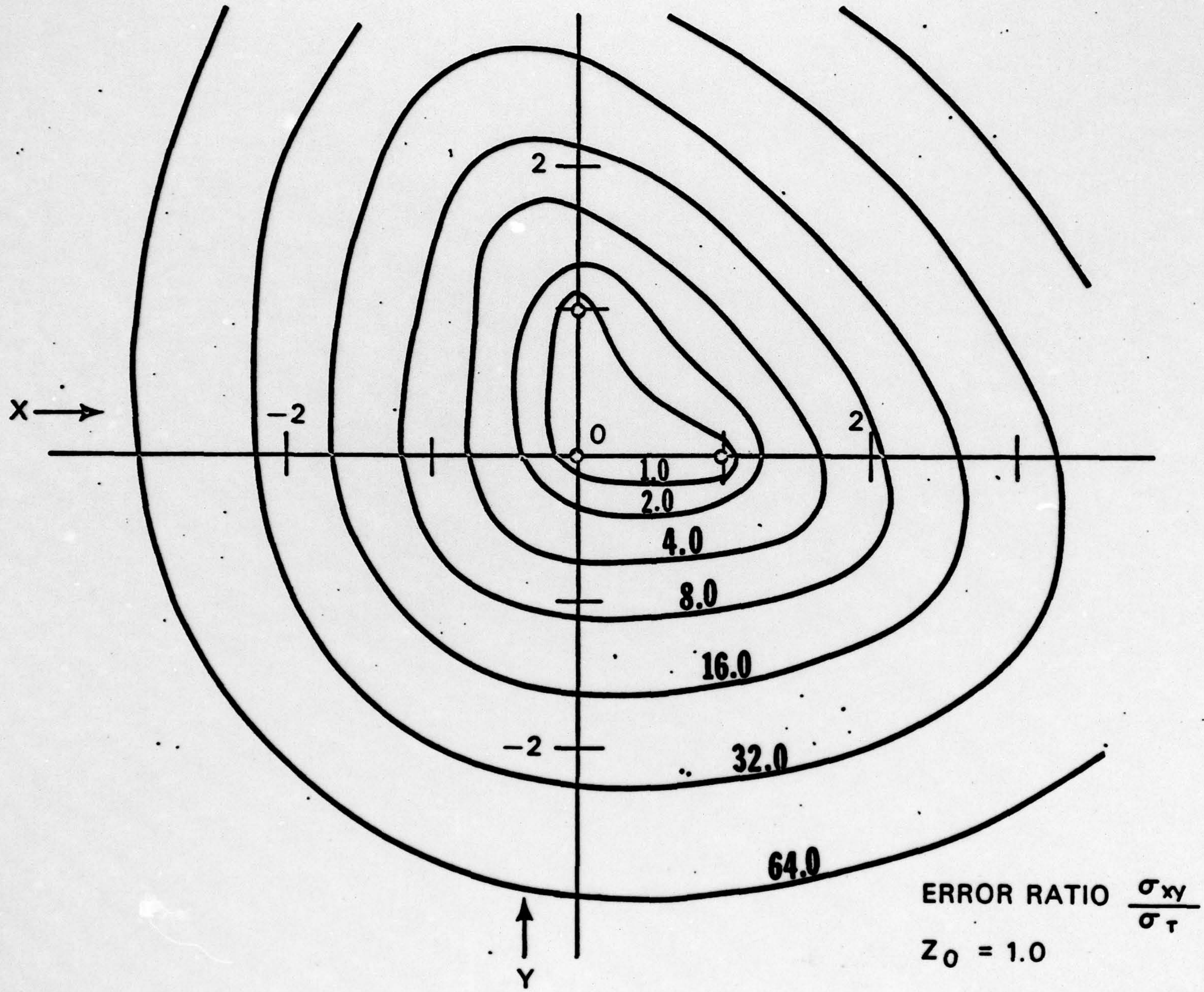

ANDERSON: FIG. 6
IPL-M-4026(U)/RAPP 12/1/76

Best
Available
Copy

APPENDIX 1

```
PROCEDURE LOCATE(T1,T2,T3,X0,Y0,Z0,R);
%**********THIS PROCEDURE ACCEPTS DATA IN THE FORM OF ESTIMATED
%LOCATIONS X0,Y0,Z0, TRAVEL TIMES T1,T2,T3 AND REFERENCE ARRAY
% R WHICH CONTAINS COORDINATES OF THE THREE REFERENCE POINTS AS
%COLUMN VECTORS.  X0,Y0,Z0 ARE REPLACED BY IMPROVED ESTIMATES.
%**********
REAL T1,T2,T3,X0,Y0,Z0;
REAL ARRAY R[0,0];
BEGIN
REAL A11,A12,A13,A21,A22,A23,A31,A32,A33,
     B11,B12,B13,B21,B22,B23,B31,B32,B33,
     DA,X,Y,Z,E1,E2,E3;
A11:=X0-R[1,1];  A12:=Y0-R[2,1];  A13:=Z0-R[3,1];%ELEMENTS OF THE 3X3
A21:=X0-R[1,2];  A22:=Y0-R[2,2];  A23:=Z0-R[3,2];%MATRIX A
A31:=X0-R[1,3];  A32:=Y0-R[2,3];  A33:=Z0-R[3,3];
%***THE B'S ARE THE COFACTORS
B11:=A22*A33-A32*A23;  B12:=-A21*A33+A31*A23;  B13:=A21*A32-A31*A22;
B21:=-A12*A33+A32*A13;  B22:=A11*A33-A31*A13;  B23:=-A11*A32+A31*A12;
B31:=A12*A23-A22*A13;  B32:=-A11*A23+A21*A13;  B33:=A11*A22-A21*A12;
DA:=A11*B11+A12*B12+A13*B13;%%THE DETERMINANT
IF ABS(DA) LSS 1 THEN DA:= SIGN(DA)-.5;%CONSTRAINT ON DETERMINANT SIZE
E1:=(T1**2-A11**2-A12**2-A13**2)/2;%COMPONENTS OF THE ERROR VECTOR
E2:=(T2**2-A21**2-A22**2-A23**2)/2;
E3:=(T3**2-A31**2-A32**2-A33**2)/2;
X:=(B11*E1+B21*E2+B31*E3)/DA;%CORRECTION INCREMENTS
Y:=(B12*E1+B22*E2+B33*E3)/DA;
Z:=(B13*E1+B23*E2+B33*E3)/DA;
X0:=X0+1.1*X;  Y0:=Y0+1.1*Y;  Z0:=Z0+1.1*Z;%CORRECTION WITH A GAIN FACTOR
END;
*
```

APPENDIX 2

```
PROCEDURE LOCATE(T1,T2,T3,X0,Y0,Z0,R);
%**********THIS PROCEDURE ACCEPTS DATA IN THE FORM OF ESTIMATED
%LOCATIONS X0,Y0,Z0, TRAVEL TIMES T1,T2,T3 AND REFERENCE ARRAY
% A WHICH CONTAINS COORDINATES OF THE THREE REFERENCE POINTS AS
%COLUMN VECTORS:  X0,Y0,Z0 ARE REPLACED BY IMPROVED ESTIMATES.
%IT INCLUDES A CONSTRAINT ON THE MAXIMUM CORRECTION INCREMENT.*******
REAL T1,T2,T3,X0,Y0,Z0;
REAL ARRAY R[0,0];
BEGIN
REAL A11,A12,A13,A21,A22,A23,A31,A32,A33,
     B11,B12,B13,B21,B22,B23,B31,B32,B33,
     DA,X,Y,Z,E1,E2,E3;
A11:=X0-R[1,1];  A12:=Y0-R[2,1];  A13:=Z0-R[3,1];%ELEMENTS OF THE 3X3
A21:=X0-R[1,2];  A22:=Y0-R[2,2];  A23:=Z0-R[3,2];%MATRIX A
A31:=X0-R[1,3];  A32:=Y0-R[2,3];  A33:=Z0-R[3,3];
%***THE B'S ARE THE COFACTORS
B11:=A22*A33-A32*A23;  B12:=-A21*A33+A31*A23;  B13:=A21*A32-A31*A22;
B21:=-A12*A33+A32*A13;  B22:=A11*A33-A31*A13;  B23:=-A11*A32+A31*A12;
B31:=A12*A23-A22*A13;  B32:=-A11*A23+A21*A13;  B33:=A11*A22-A21*A12;
DA:=A11*B11+A12*B12+A13*B13;%%THE DETERMINANT
IF ABS(DA) LSS 1 THEN DA:= SIGN(DA)-.5;%CONSTRAINT ON DETERMINANT SIZE-
R1:=A11**2+A12**2+A13**2;%RANGES TO X0,Y0,Z0.
R2:=A21**2+A22**2+A23**2;
R3:=A31**2+A32**2+A33**2;
E1:=(T1**2-R1)/2;%COMPONENTS OF THE ERROR VECTOR
E2:=(T2**2-R2)/2;
E3:=(T3**2-R3)/2;
LIM1:=E1**2/2/(R1+T1**2);%ESTIMATING THE TIME DELAY ERRORS
LIM2:=E2**2/2/(R2+T2**2);
LIM3:=E3**2/2/(R3+T3**2);
LIM1:=MAX(LIM1,LIM2);
LIM1:=MAX(LIM1,LIM3);%MAXIMUM SQUARED TIME DELAY ERROR
X:=(B11*E1+B21*E2+B31*E3)/DA;%CORRECTION INCREMENTS
Y:=(B12*E1+B22*E2+B33*E3)/DA;
Z:=(B13*E1+B23*E2+B33*E3)/DA;
R:=X**2+Y**2+Z**2;
 FACT:=SQRT(LIM1/R)*3;%CONSTRAINT FACTOR
IF R GEQ 10*LIM1 THEN BEGIN X:=X*FACT;Y:=Y*FACT;Z:=Z*FACT;END;
X0:=X0+1.1*X;  Y0:=Y0+1.1*Y; Z0:=Z0+1.1*Z;%CORRECTION WITH A GAIN FACTOR
END;
```

APPENDIX 3

```
REAL PROCEDURE PHASETIME(CO,QUAD,OMEGA);
REAL CO,QUAD,OMEGA;
%****************THIS ROUTINE CONVERTS CO AND QUAD PHASE
% COMPONENTS TO A TIME DELAY MODULO ONE PERIOD.  THE
% MAIN PROGRAM MUST SET UP THE LOOKUP TABLE WITH STATEMENTS
% SUCH AS ----------------------
%   REAL ARRAY ARCSINE[-50:50];  REAL I;
%   FOR I := -50 STEP 1 UNTIL 50 DO ARCSINE[I]:=ARCSIN(I/50.);
%*****************************************************
BEGIN
REAL MOD,T;
MOD:= SQRT(CO**2+QUAD**2);
CO:=CO*50/MOD;  QUAD:=QUAD*50/MOD;
IF ABS(CO) GEQ .707 THEN
     IF CO GTR 0 THEN
          T := ARCSINE[QUAD]
       ELSE T := SIGN(QUAD)*(3.14159-ABS(ARCSINE[QUAD]))
  ELSE T := SIGN(QUAD)*(1.57080-ARCSINE[CO]);
PHASETIME := T/OMEGA;
END;
```

```
PROCEDURE ROTATE(CO,QUAD,RJ,KAY,SHIFT);
REAL CO,QUAD,RJ,KAY,SHIFT;
%**********ROTATION OF COMPONENTS CO AND QUAD BY THE PHASE SHIFT
% OVER PATH RJ AT WAVENUMBER KAY AND BY INSTRUMENTAL PHASE SHIFT
% "SHIFT" IN RADIANS.  THE MAIN PROGRAM MUST SET UP A SINE LOOK
% UP TABLE AS FOLLOWS--------
%     REAL ARRAY SINE[0:160];  REAL I;
%     FOR I := 0 STEP 1 UNTIL 160 DO
%     SINE[I] := SIN(3.14159/I/64);
%**********
BEGIN
REAL ALPH,BET,CO1,QUAD1;
INTEGER TRUNC;
TRUNC := INT((RJ*KAY+SHIFT)*20.3718);
TRUNC := TRUNC - TRUNC MOD 128;
ALPH := SINE[TRUNC+32];
BET := SINE[TRUNC];
CO1 := CO*ALPH + QUAD*BET;
QUAD1 := QUAD*ALPH - CO*BET;
CO := CO1;  QUAD := QUAD1;
END;
```

9 (?)

DISTRIBUTION LIST

Director
Advanced Research Projects Agency
1400 Wilson Boulevard
Arlington, Virginia 22209 (3)

Office of Naval Research Branch Office
1030 E. Green Street
Pasadena, California 91101 (1)

Mr. T.F. Locas
ONR Resident Representative
University of California, San Diego
P.O. Box 109
La Jolla, California 92037 (1)

Cdr. Donald D. Pizinger, Code, 212
Office of Naval Research
Department of the Navy
Arlington, Virginia 22217 (1)